

Modeling of a Synchrophasor Measurement Unit in an Electromagnetic Transient Simulation Program

Dinesh Rangana Gurusinghe, Athula D. Rajapakse, Dharshana Muthumuni

Abstract— The process of development of synchrophasor based wide area control applications heavily rely on simulations. When using synchrophasors for applications that involve fast phenomena, it is important to accurately model the phasor measurement unit (PMU). The accuracy and the consistency of PMU performance during transient conditions is achieved by using P-class and M-class backend filters as stipulated in the recently published IEEE standard C37.118.1-2011. Phasor values reported by a PMU during transients depend on the characteristics of these filters. Use of electromagnetic transient (EMT) simulation is necessary to represent this type of details. Thus, it is necessary to develop realistic model of a PMU for complete simulation of synchrophasor based wide area control applications in EMT programs.

Keywords: Phasor measurement unit (PMU), Synchrophasors, Electromagnetic transient simulation, PMU performance class filters, Phasor data concentrator.

I. INTRODUCTION

SYNCHROPHASOR measurements, when combined with advanced telecommunication infrastructure, enables real-time observation of the dynamics of an interconnected power system spread over a large geographical area. This makes it possible the design of wide area control schemes against disturbances that could lead to catastrophic failures [1]. Synchrophasor technology allows measurement of phase angles and magnitudes of sinusoidal voltages and currents at different locations of the network with respect to a common reference using the phasor measurement units (PMUs) [2]. PMUs send the measured synchrophasor data through a communication network to a phasor data concentrator (PDC). The PDC collects the data from different PMUs, time align them and send the collected data to local applications, higher level PDCs and archives [3], [4]. PMUs are considered one of the most important measuring devices in future of power systems [5].

Simulations play an important role in the process of development of synchrophasor based wide area control applications. When using synchrophasors for applications that involve fast phenomena such as wide area control against

transient stability, or systems that contain complete feedback control loops such as wide area oscillation damping controllers [6], it is essential to precisely model the synchrophasor extraction process. The recently published IEEE standard C37.118.1-2011 [7] ensures the accuracy and the consistency of PMU performance during transient conditions with the aid of backend performance class filters namely; P-class and M-class. Transient performances and accuracy of PMU measurements heavily rely on the characteristics of these filters. Electromagnetic transient (EMT) simulation is the most preferred option to represent this type of details.

A number of commercial EMT simulation programs such as ATP program, MicroTran, PSCAD/EMTDC, NETOMAC, and Power System Toolbox are widely used to simulate transient phenomenon of power system [8]. In these EMT programs, phasors are generally extracted using the standard discrete Fourier transform (DFT) or fast Fourier transform (FFT), but they do not accurately represent the synchrophasor extraction process satisfying the requirements of C37.118.1-2011. In addition, these phasor extraction models cannot be used to represent PMUs as their output reporting rate incorrectly simulate the actual PMU behavior. Furthermore, neither of models comprise with communication interface, which is essential to develop synchrophasor network in EMT simulations.

The objective of this paper is to implement a detailed model of a PMU with an appropriate communication interface in the industry standard EMT simulation program. The simulations are performed to highlight the transient performances of the developed PMU model in comparison to the standard FFT techniques. This paper is organized as follows. The PMU modeling of the paper is discussed in Section II. Section III is devoted to simulation results and discussion. It assesses performance and accuracy of the PMU model with a simple transient stability application, which quantifies the impact of simply taking the generator terminal voltage angle from the PMU measurements to represent the generator rotor angle in the assessment of power system rotor angle instabilities. Finally, in Section IV, the main conclusions of this paper are presented.

II. PMU MODELING

The signal processing model of a PMU implemented in PSCAD/EMTDC is shown in Fig. 1. The input voltage or/and current waveforms are fed to the frontend anti-aliasing filter, where high frequency interference signals are eliminated. The analogue to digital (A/D) converter digitizes the signal at fixed

D. R. Gurusinghe and A. D. Rajapakse are with the Dept. of Electrical and Computer Engineering, University of Manitoba, Winnipeg, MB, R3T5V6, Canada (e-mail: umgurusi@cc.umanitoba.ca; athula@ee.umanitoba.ca).

D. Muthumuni is with the Manitoba HVDC Research Centre, Winnipeg, MB, R3P1A3, Canada (e-mail: dharshana@hvdc.ca).

sampling rate synchronized to a global position system (GPS) clock, which provides coordinated universal time (UTC). DFT algorithm is a popular approach, where samples are multiplied by the power system nominal frequency quadrature oscillator to extract real and imaginary components of the phasor. Finally, the real and imaginary components of the phasor are passed through either P-class or M-class backend performance class filter to achieve required accuracy under dynamic conditions. In a PMU, final phasor values are used to estimate secondary quantities such as frequency, rate of change of frequency (ROCOF), real/reactive power.

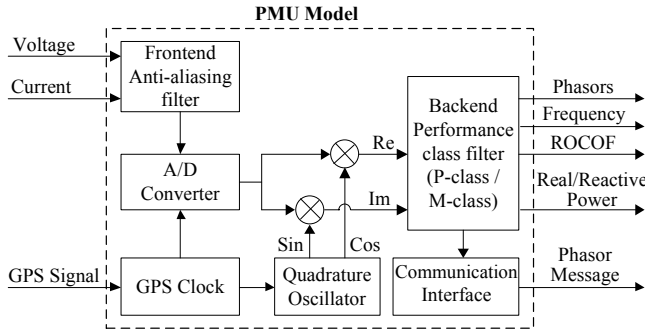


Fig. 1. The signal processing model of a PMU implemented in PSCAD

In this paper, sixth order Butterworth low-pass filter with cut-off frequency at one half of sampling frequency is used as a frontend anti-aliasing filter. The sampling rate, N_s of the PMU model can be selected from 8 to 96 samples/cycle, where higher sampling rates slightly increase the accuracy.

The DFT phasor extraction and the backend performance class filtering process is mathematically represented in (1), where the phasor, X of signal x at the n^{th} sampling point is given as [7],

$$X(n) = \frac{\sqrt{2}}{G_W} \cdot \sum_{k=-N/2}^{+N/2} x(n+k) \cdot \exp\left[-\frac{2\pi(n+k)}{N_s}\right] \cdot W(k) \quad (1)$$

where N is the filter order, which can be obtained by matching frequency response characteristics given in [7], $W(k)$ are filter coefficients and G_W is the backend filter gain given by,

$$G_W = \sum_{k=-N/2}^{+N/2} W(k) \quad (2)$$

The coefficients of the P-class and M-class filters as specified in [7] are given in (3) and (4) respectively.

$$W(k) = 1 - \frac{2}{N+2} |k| \quad (3)$$

$$W(k) = \text{sinc}\left(\frac{4\pi F_{fr} k}{f_0 N_s}\right) h(k) \quad (4)$$

where $k = -N/2 :+ N/2$ (integers), f_0 is the nominal power system frequency (50 or 60 Hz), $h(k)$ is the Hamming function and F_{fr} is the filter reference frequency specified in [7].

Once phasors are known, frequency can be estimated by taking first numerical derivative of the phase angle while ROCOF can be obtained by taking second numerical derivative of the phase angle. If both voltage and current signals are fed to the PMU model it can determine real and reactive power measurements.

The frontend anti-aliasing filter and the backend performance class filter introduce delays to the signal. These delays and other processing delays of the PMU model can be rectified with the aid of proper time-stamps. The UTC corresponding to the beginning of the simulation is provided as a parameter input to the PMU model. If this is not provided, the PMU model can extract an initial UTC based on the computer clock. When a simulation is in progress, the PMU model determines UTC from the initial UTC and the simulation time. The time-stamp is then determined by deducting filter group delays and other processing delays.

Even though the PMU estimates phasors at every sampling point, all the estimates are not reported. Number of phasors reported per second depends on the selected standard reporting rate, which is an integer submultiple of the system nominal frequency [7]. Thus, the measurements are picked at every reporting point and kept unchanged until the next reporting time arrives.

In actual PMU, phasors and other interested quantities including the PMU identification number are combined to make a data frame according to the format prescribed in the standard [9]. This data frame is sent out as a data packet using a communication protocol such as transmission control protocol/internet protocol (TCP/IP). In the simulation, this data frame can be represented as a large hexadecimal number and sent to the PDC at every reporting point. However, this hexadecimal number could be very large depending on the number of phasors and other data sent in the phasor message. Even a 64-bit computer system cannot handle such a large hexadecimal and therefore, this large hexadecimal number is split into several small numbers of manageable size and sent as parallel messages. A communication interface is provided in the PMU model output these messages containing the synchrophasor data. These parallel messages can be combined and decoded into actual measurements at PDC. A separate research is underway to develop a communication network simulation model, however, modeling of the communication network and the PDC are beyond the scope of this paper.

The phasor measurement errors are computed using the concept of total vector error (TVE) and frequency error (FE) defined in [7]:

$$TVE(n) = \frac{|x_a(n) - x_m(n)|}{|x_a(n)|} \quad (5)$$

$$FE(n) = |f_a(n) - f_m(n)| \quad (6)$$

where $x_a(n)$, $x_m(n)$ are the actual and the measured phasors while $f_a(n)$, $f_m(n)$ are the actual and the measured frequencies.

The existing FFT model in PSCAD/EMTDC is based on the standard FFT technique, which computes the DFT calculations more rapidly [10]. In this approach, DFT of size p divides into two smaller DFTs of size $p/2$; the even-indexed inputs and the odd-indexed inputs and then two outputs are combined to produce the complete DFT. This technique is known as Cooley-Tukey (radix-2) algorithm [11]. The FFT model comprises with an anti-aliasing filter and a frequency tracker, they can either be enabled or disabled, depends upon an application. In addition to the fundamental phasors, the

FFT model can measure harmonics from 2nd to 255th, where the sampling rate is automatically increased according from 16 to 512 samples/cycle [10] depending on the number of harmonics required.

III. SIMULATION RESULTS AND DISCUSSION

A. PMU Model Evaluation

Performances and accuracy of the PMU model need to be evaluated under a variety of conditions that are specified in [7]. Signal frequency, measurement bandwidth, linear frequency ramp and step response tests are executed to assess compliance of the PMU model in simulation environment. In this paper, 60 Hz power system is considered in presenting simulation results, but the PMU model demonstrates similar performances for 50 Hz power system as well. Test results illustrate performances at a sampling rate of 8 samples/cycle and a reporting rate of 60 frames/s (the highest reporting rate). In [4], it was found that if a PMU fulfills performances at the highest reporting rate, it satisfies the accuracy requirements at lower reporting rates. Tests are conducted by varying one parameter in the input signal while keeping other factors constant for the period of measurement. The maximum TVE and FE observed during the test period are noted. Errors of the PMU model are compared with the existing FFT model in PSCAD/EMTDC. Time stamps for the FFT results are assigned based on the simulation time at which the particular phasor is output by the FFT model.

1) Signal frequency :

In the signal frequency test, the input signal frequency, f in (7) is varied from 55 Hz to 65 Hz with a step resolution of 1 Hz to simulate the frequency deviation in the power system from the nominal system frequency.

$$x(t) = X_m \cos(2\pi ft) \quad (7)$$

where X_m is the amplitude of the sinusoidal waveform. The maximum percentage TVE on logarithmic scale (base 10) and the maximum FE are shown in Fig. 2. The specified range of frequency for P-class is only from 58-62 Hz.

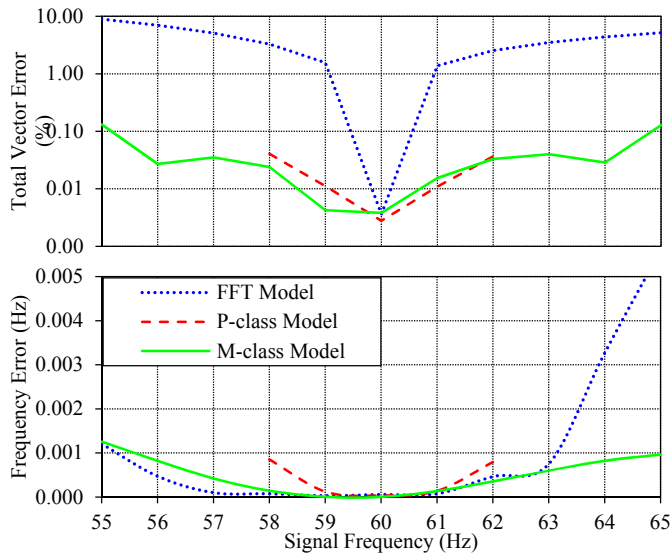


Fig. 2. Signal frequency response

It is observed that the PMU model satisfies both the TVE requirements ($< 1\%$) and the FE requirements (< 0.005 Hz). However, the existing FFT model satisfies neither of them. It should be noted that frequency tracking in the FFT model was enabled during the test.

2) Measurement bandwidth :

The amplitude or/and phase angle of a sinusoidal waveform is modulated to simulate oscillations in the power system. The test signal is given in (8) as per [7].

$$x(t) = X_m [1 + 0.1 \cos(2\pi f_m t)] \cos[2\pi f_0 t + 0.1 \cos(2\pi f_m t - \pi)] \quad (8)$$

where f_0 is the nominal system frequency and f_m is the modulation frequency, which is varied from 0.1 to 5 Hz. The maximum percentage TVE on logarithmic scale (base 10) and the maximum FE are shown in Fig. 3. The specified range of modulation frequency for P-class is only from 0.1-2 Hz.

In the PMU model, the TVE remains less than 0.25% and the FE remain 0.2 Hz throughout the expected modulation frequency range. However, the existing FFT model can satisfy the measurement bandwidth TVE requirements only up to a modulation frequency of 3 Hz. Beyond that the maximum TVE rises above 3%. The FE of FFT model is always beyond the specified limit of 0.3 Hz.

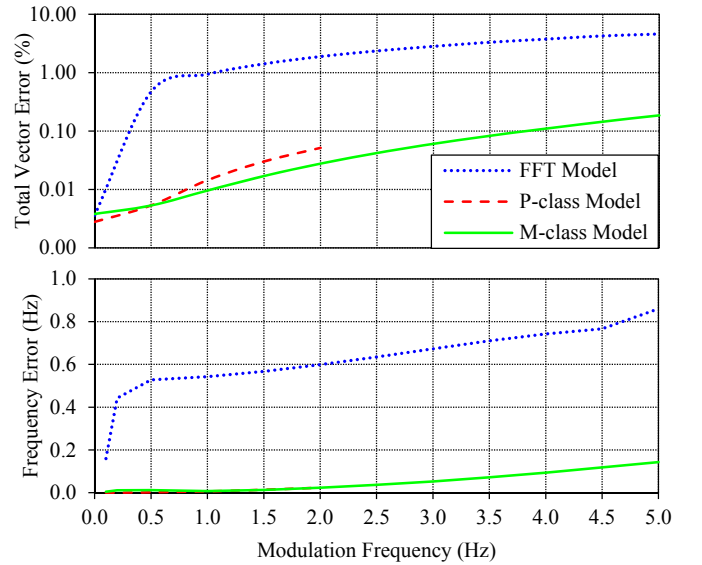


Fig. 3. Magnitude and phase angle modulation response

3) Linear frequency ramp :

The input signal frequency is changed at a linear rate starting from its nominal value (60 Hz) to simulate sudden system imbalances. The test signal is given in (9) as per [7].

$$x(t) = X_m \cos(2\pi f_0 t + \pi R_f t^2) \quad (9)$$

where R_f is the signal ramp rate, which is varied for negative ramps up to -1.0 Hz/s (60 Hz-55 Hz) and for positive ramps up to $+1.0$ Hz/s (60 Hz-65 Hz). The maximum percentage TVE on logarithmic scale (base 10) and the maximum FE are shown in Fig. 4. The specified range of frequency ramp for P-class is only from 58-62 Hz. The developed PMU model satisfies the TVE requirements ($< 0.25\%$) throughout the expected frequency ramp rates. However, the PMU model can

only satisfy P-class FE requirement (0.01 Hz) whereas M-class maximum FE is 0.011 Hz, which is beyond the specified value (0.005 Hz). The existing FFT model cannot satisfy both TVE and FE specifications as per [7].

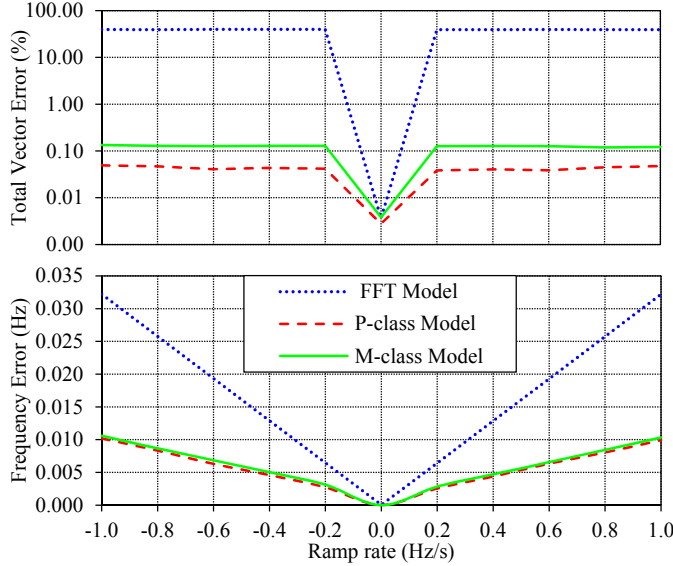


Fig. 4. Linear frequency ramp response

Table I summarizes results of the signal frequency, the measurement bandwidth and the frequency ramp test for the existing FFT model in PSCAD/EMTDC and the developed model with P-class and M-class performance filters.

TABLE I
TVE AND FE RESULTS

Influence Quantity	PMU Model	Max TVE (%)	Max FE (Hz)
Signal frequency	FFT Model	8.92	0.006
	P-class Model	0.04	0.001
	M-class Model	0.13	0.001
Measurement bandwidth	FFT Model	4.59	0.860
	P-class Model	0.05	0.023
	M-class Model	0.18	0.143
Linear frequency ramp	FFT Model	39.83	0.032
	P-class Model	0.05	0.010
	M-class Model	0.13	0.011

4) Step response :

The step test simulates various power system switching events. A unit step function $u(t)$ is applied to the input signal magnitude or phase angle to simulate magnitude step or phase angle step respectively. The test signal for magnitude step is given in (10) while same for phase angle step is given in (11) as per [7].

$$x(t) = X_m [1 + 0.1u(t)] \cos(2\pi f_0 t) \quad (10)$$

$$x(t) = X_m \cos \left[2\pi f_0 t + \frac{\pi}{18} u(t) \right] \quad (11)$$

The step is introduced at a precise time. The response time, delay time and maximum overshoot/undershoot are determined as specified in [7]. The equivalent sampling approach [3], [7] is used to realize the required measurement resolution as response time and delay time are small compared to the PMU reporting interval. Fig. 5 illustrates magnitude, TVE and FE responses for the magnitude step. All graphs are

plotted on the same time scale. The corresponding responses for the phase angle step are shown in Fig. 6.

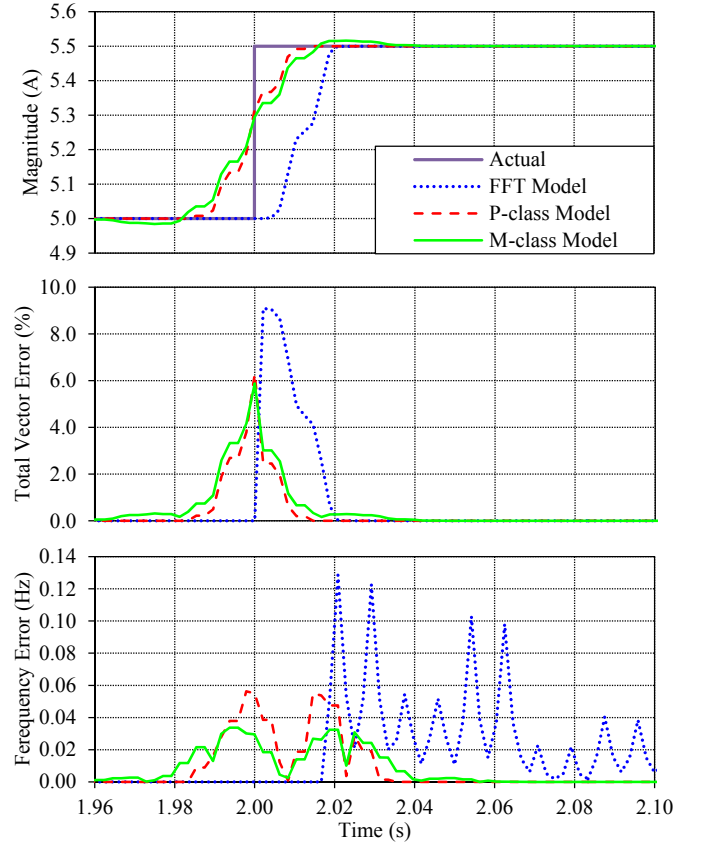


Fig. 5. Waveforms of magnitude positive step response

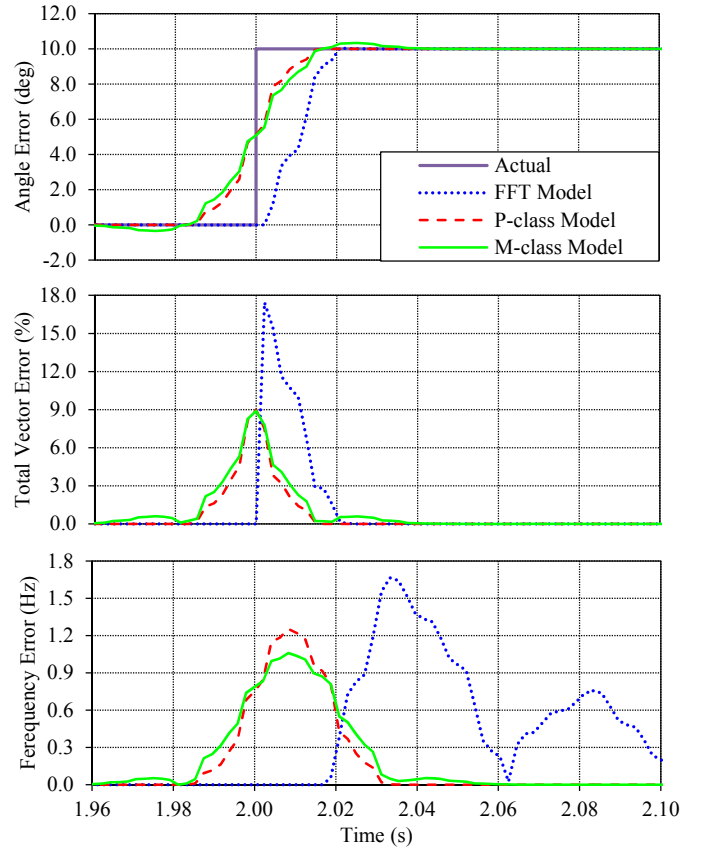


Fig. 6. Waveforms of phase angle positive step response

It is observed that the developed PMU model fulfills the step response requirements of [7]. However, the existing FFT model only satisfies the response time and the maximum overshoot/undershoot value necessities, but exceeds the delay time and the frequency response time specification. The TVE response time, delay time, maximum overshoot/undershoot and frequency response time for each of the test cases are provided in Table II.

TABLE II
STEP CHANGE PERFORMANCE

Influence Quantity	PMU Model	Response Time (ms)	Delay Time (ms)	Max. Overshoot / Undershoot (% of step)	Frequency Response Time (ms)
10% magnitude positive step	FFT Model	18.58	12.27	0.00	137.98
	P-class Model	18.92	1.04	0.00	48.65
	M-class Model	23.09	1.05	3.22	59.36
10% angle positive step	FFT Model	19.71	11.20	0.58	297.53
	P-class Model	28.65	0.56	0.00	50.73
	M-class Model	28.82	0.56	3.43	97.48

B. Transient Stability Application

Rotor angles of generators are direct indicators of the transient instabilities and highly useful in the real time transient stability assessment [6]. The rotor angle, δ , of a generator can be estimated from the PMU measurements of terminal quantities (voltage, E_t and current, I_t) with the knowledge of the quadrature-axis reactance, x_q , the armature resistance, R_a , of the generator as:

$$\delta = \text{angle}(E_t + I_t R_a + j I_t x_q) \quad (12)$$

However, it is practically complicated to find the quadrature-axis reactance and the armature resistance. Therefore, the generator terminal voltage angle obtained from the PMU measurements is used to approximately represent the generator rotor angle in the assessment of power system rotor angle instabilities. The PMU model developed in this paper is used to investigate the validity of the above approximation.

Transient stability of a one machine to infinite bus (OMIB) system shown in Fig. 7 is simulated with a 555 MVA, 24 kV, 60 Hz, three-phase, 2-pole synchronous generator given in [12]. The parameters of the generator, its excitation system with automatic voltage regulator (AVR) and power system stabilizer (PSS) are given in Appendix. The generator terminal voltage and current are fed to a PMU model, which is located at the generator terminal bus.

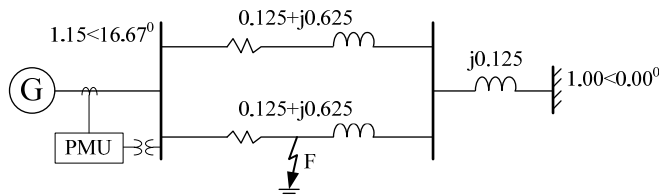


Fig. 7. OMIB system with the initial steady-state power flow solution

The OMIB system is modeled with the standard synchronous generator and transmission line components. The developed M-class PMU model is used to obtain synchrophasor measurements at the generator terminal with a sampling rate of 8 samples/cycle and a reporting rate of 60 frames/s.

The simulation is started with the initial steady-state power flow solution. When the generator delivers 500 MVA at 0.9 power factor (lagging) the initial steady-state power flow solution provides the generator terminal voltage as $1.15 \angle 16.67^\circ$. A three-phase bolted fault is applied at the midpoint (location F) of one of the parallel transmission lines and the fault is cleared by removing the faulted line. It is observed that the power system is stable when the fault clearing time, t_c , is less than or equal 0.49 seconds whereas the power system is unstable when it is greater than 0.49 seconds. Thus, the critical clearing time of the power system is about 0.49 seconds.

Fig. 8 shows the variations of the rotor angle obtained from the standard generator model in PSCAD/EMTDC, the rotor angle derived from the PMU measurements as per (12), and the terminal voltage angle obtained from the PMU model for three different scenarios namely; stable case without a PSS, stable case with a PSS, and unstable case. All graphs are plotted on the same time scale. It is observed that the rotor angle is steady during the pre-fault and oscillates after clearing the fault. The oscillation of the rotor angle sustains a significant period and it can be rapidly damped with the aid of a PSS.

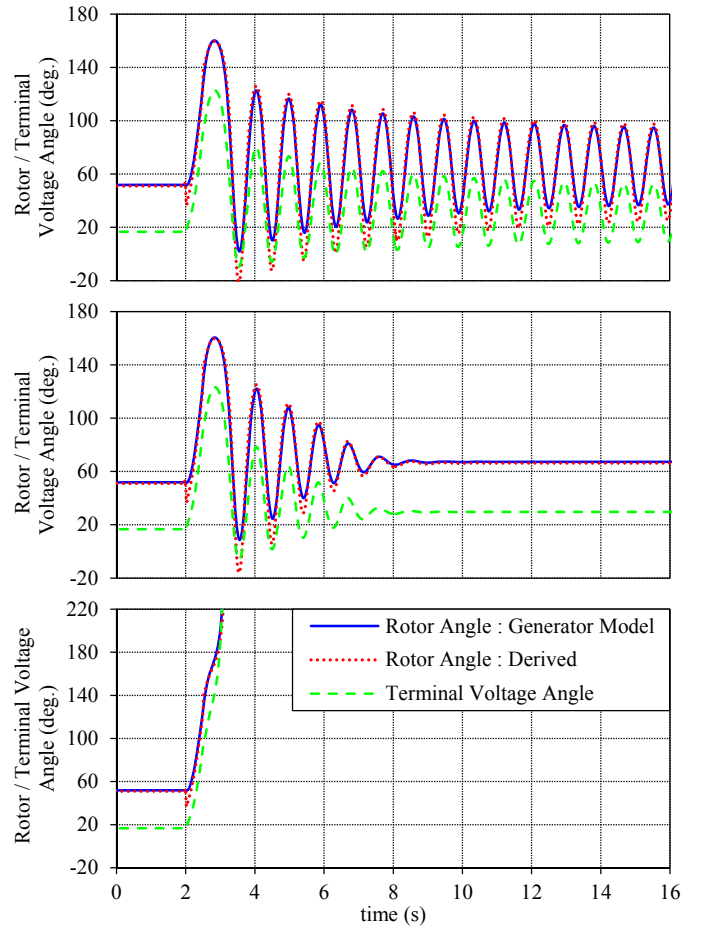


Fig. 8. Rotor / terminal voltage angle variation with time ($t_c = 0.49$ sec. without a PSS : stable, $t_c = 0.49$ sec. with a PSS : stable, and $t_c = 0.50$ sec. : unstable)

The generator model provides the initial steady-state rotor angle as 51.85° while the derived rotor angle from (12) also

provides a similar value. The derived rotor angle peak values are different during the transient but the pattern of variation is very similar to the variation of actual rotor angle. Furthermore, it is visible that the terminal voltage angle variation with time also follows the standard generator model rotor angle variation in all three scenarios. Although the pattern of variation is similar, the values of the terminal voltage angle are different from the actual rotor angle. Therefore, the generator terminal voltage angle obtained from the PMU measurements may be appropriate to represent the generator rotor angle in the assessment of power system rotor angle instabilities, if only the pattern of variation is important.

IV. CONCLUSIONS

In this paper, a detailed model of a PMU with an appropriate communication interface is implemented in an industry standard EMT simulation program. The simulations were performed to highlight the transient performances of the developed PMU model in comparison to the standard FFT techniques. The standard FFT models failed to achieve TVE and FE requirements of the latest IEEE synchrophasor standard C37.118.1-2011 [7]. The new PMU model implemented with P-class and M-class performance filters achieved both TVE and FE requirements of [7]. In addition, a communication interface to the PMU model is provided to enable the modeling of a PMU communication network in the simulation. The developed PMU model is applied to analyze the validity of using the generator terminal voltage angle from PMU measurements to represent the generator rotor angle, if only the pattern of variation is important to assess power system rotor angle instabilities.

V. APPENDIX

Synchronous generator parameters:

The synchronous generator is represented by an equivalent circuit whose parameters in per unit on 555 MVA base are as follows [12].

$$\begin{array}{llll}
 K_D = 0 & H = 3.5 & & \\
 L_{ad} = 1.66 & L_{aq} = 1.61 & L_l = 0.15 & R_a = 0.003 \\
 L_{fd} = 0.165 & R_{fd} = 0.0006 & L_{1d} = 0.1713 & R_{1d} = 0.0284 \\
 L_{1q} = 0.7252 & R_{1q} = 0.00619 & L_{2q} = 0.125 & R_{2q} = 0.02368
 \end{array}$$

Excitation system:

The excitation system model with AVR and PSS [12] shown in Fig. 9 is replicated in this paper.

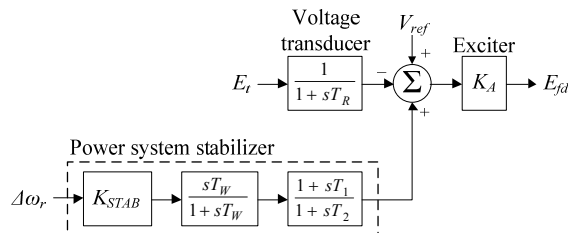


Fig. 9. Excitation system with AVR and PSS [12]

$$\begin{array}{llll}
 K_A = 200 & T_R = 0.02s & & \\
 K_{STAB} = 9.5 & T_W = 1.4s & T_l = 0.154s & T_2 = 0.033s
 \end{array}$$

VI. REFERENCES

- [1] E. O. Schweitzer III, D. Whitehead, G. Zweigle and K. G. Ravikumar, "Synchrophasor-based power system protection and control applications," in *Proc. 2010 Texas A&M Conf. for Protective Relay Engineers*, 2010.
- [2] A. G. Phadke and J.S. Thorp, *Synchronized Phasor Measurements and Their Applications*, New York: Springer, 2008.
- [3] K. Martin, T. Faris and J. Hauer, "Standardized testing of phasor measurement units," in *Proc. 2006 Fault and Disturbance Analysis Conf.*, pp. 1-21.
- [4] D. R. Gurusinge, A. D. Rajapakse and K. Narendra, "Evaluation of steady-state and dynamic performance of a synchronized phasor measurement unit," in *Proc. 2012 IEEE Electrical Power and Energy Conf.*, pp. 57-62.
- [5] R. F. Nuqui, "State Estimation and Voltage Security Monitoring Using Synchronized Phasor Measurements," Ph.D. dissertation, Dept. Electrical Eng., Virginia Polytechnic Institute and State University, Blacksburg, Virginia, 2001.
- [6] P. Kundur, J. Paserba, V. Ajarapu, G. Andersson, A. Bose, C. Canizares, N. Hatziaargyriou, D. Hill, A. Stankovic, C. Taylor, T. Cutsem and V. Vittal, "Definition and classification of power system stability," *IEEE Trans. Power Systems*, vol. 19, pp. 1387-1401, May 2004.
- [7] IEEE Standard for Synchrophasor Measurements for Power Systems, IEEE Standard C37.118.1-2011, Dec. 2011.
- [8] N. Watson and J. Arrillaga, *Power Systems Electromagnetic Transients Simulation*, The Institution of Engineering and Technology, London, UK, 2007.
- [9] IEEE Standard for Synchrophasor Data Transfer for Power Systems, IEEE Standard C37.118.2-2011, Dec. 2011.
- [10] PSCAD User's Guide, [Online]. Available: https://hvdc.ca/uploads/ck/files/reference_material/PSCAD_User_Guide_v4_3_1.pdf.
- [11] P. Duhamel and M. Vetterli, "Fast Fourier transforms: a tutorial review and a state of the art", *Journal of Signal Processing*, vol. 19, pp. 259-299, Apr. 1990.
- [12] P. Kundur, *Power System Stability and Control*, New York: McGraw-Hill, 1994.